PROCEEDINGS OF SPIE

SPIEDigitalLibrary.org/conference-proceedings-of-spie

# Development of high efficiency and wide acceptance angle holographic solar concentrators for breakthrough photovoltaic applications

Marta Morales-Vidal, Tomás Lloret, Belén Nieto-Rodríguez, José Carlos García-Vázquez, Kheloud Berramdane, et al.

Marta Morales-Vidal, Tomás Lloret, Belén Nieto-Rodríguez, José Carlos García-Vázquez, Kheloud Berramdane, Eva M. Calzado, Inmaculada Pascual, "Development of high efficiency and wide acceptance angle holographic solar concentrators for breakthrough photovoltaic applications," Proc. SPIE 12574, Holography: Advances and Modern Trends VIII, 125740C (31 May 2023); doi: 10.1117/12.2665633

SPIE.

Event: SPIE Optics + Optoelectronics, 2023, Prague, Czech Republic

# Development of high efficiency and wide acceptance angle holographic solar concentrators for breakthrough photovoltaic applications

Marta Morales-Vidal[a, b], Tomás Lloret[b], Belén Nieto-Rodríguez[b], José Carlos García-Vázquez[a], Kheloud Berramdane[a], Eva M. Calzado[a], and Inmaculada Pascual[a, b]

[a]Instituto Universitario de Física Aplicada a las Ciencias y las Tecnologías, Universidad de Alicante, Carretera San Vicente del Raspeig s/n, 03690 San Vicente del Raspeig, Spain
[b]Departamento de Óptica, Farmacología y Anatomía, Universidad de Alicante, Carretera San Vicente del Raspeig s/n, 03690 San Vicente del Raspeig, Spain

## ABSTRACT

Solar concentrator systems represent an important challenge in our society for outstanding photovoltaic (PV) applications. Fresnel lenses or parabolic mirrors concentrate sunlight in a small solar cell surface. On the one hand, Fresnel lenses have an exceedingly small acceptance angle and require expensive tracking systems to follow the path of the Sun. On the other hand, conventional parabolic mirrors need periodic maintenance of the surface reflectivity. Holographic optical elements (HOEs) represent a suitable alternative to Fresnel lenses and solar reflectors, they are cheaper and more versatile. Particularly, multiplexed holographic solar concentrators (HSCs) give an insight into promising possibilities for Building-Integrated Concentrating PV (BICPV). A good trade-off between wide acceptance angle and high diffraction efficiency represents an important milestone in the area. Our research group obtained the higher acceptance angle in a multiplexed HSC design (Morales et. al. Opt. Express 30, 25366 (2022)). This design was composed of seven holographic multiplexed lenses in Biophotopol material with thick thickness, 197 $\mu$m. In the present work, more efficient holographic solar concentrators than previous works are shown. As far as we know, it has been obtained the best trade-off between high efficiency and wide acceptance angle HSC-PV solar cell systems.

**Keywords:** Photovoltaic energy, multiplexed lenses, low-toxicity photopolymer, free-tracking system, building-integrated concentrating photovoltaic

## 1. INTRODUCTION

One of the strategic lines of 2030 Horizon is to develop affordable and clean energy. Solar energy represents a clean and renewable alternative to the overexploitation and excessive use of non-renewable energies. The high efficiency and high cost of cells in the 1980s were the most important motivation to develop photovoltaic (PV) concentrators during the last decades. The first design and development of an experimental PV concentrator module was published in 1984 at Sandia laboratory in New Mexico (USA).[1] Since then, innovative technologies and designs have been developed.[2,3] Today, the most widespread technologies for concentrating light are Fresnel lenses and reflective elements.[4] On the one hand, Fresnel lenses have a high concentration ratio, but have a very small acceptance angle, around 1°. It requires cooling and expensive tracking systems to follow the path of the sun from sunrise to sunset. On the other hand, reflective elements (so-called first mirrors) have high optical efficiency, but are expensive and must be protected from moisture and mechanical stresses that cause corrosion.[5]

Holographic optical elements (HOEs) can focus, redirect or reflect incoming light to different PV cells and thus efficiently convert solar energy into electrical energy.[6] The development of holographic technology can increase the small acceptance angle of traditional solar concentrators.[7,8] The acceptance angle is defined as the maximum angle at which incoming sunlight can be captured by a solar concentrator. Maximimizing the acceptance angle

Further author information: (Send correspondence to M.M.V.)
M.M.V.: E-mail: marta.morales@ua.es, Telephone: 96 590 34 00

Holography: Advances and Modern Trends VIII, edited by Antonio Fimia, Miroslav Hrabovský, Proc. of SPIE Vol. 12574, 125740C
 · 0277-786X · doi: 10.1117/12.2665633

of the concentrator is desirable in practical systems and can be achieved by using nonimaging optics. Therefore, holographic solar concentrators have great potential to diffract light at large offset angle and also offer great possibilities for multiplexing a large number of optical elements in the same thin device.[9,10] So far different research groups have developed different holographic solar concentrators.[11–15] The maximum acceptance angle obtained with double layer or multiplexed lenses range between 30° to 50°,[11,13,15] while the maximum diffraction efficiencies have been obtained with multilayer devices or with a small number of multiplexed holographic lenses (HLs).[12,14]

In this work we will present, to the best of our knowledge, the best low-toxicity multiplexed holographic solar concentrator obtained so far. First, four peristrophic multiplexed holographic solar concentrators will be recorded by rotating the sample in each new holographic configuration 7.4°, each of them is based on seven HLs recorded and superimposed on different spots of the same plate. It will be analyzed and represented the slant obtained in each holographic configuration. Secondly, the reconstruction of the holographic concentrators under red and sunlight as a function of different incidence angles will be studied. Finally, future projections of this work for breakthrough photovoltaic applications will be discussed.

## 2. EXPERIMENTAL METHODS

### 2.1 Multiplexed Holographic Concentrators

The solar concentrators studied in this work were fabricated by holographic methods on an environmentally friendly photopolymer called Biophotopol and supported on glass plates. The prepolymer solution in water is composed of 13.3 w/V poly(vinyl alcohol) (PVA) as inert binder polymer (Mw $\sim$ 130000), degree of hydrolysis = 87.7%), sodium acrylate ($C_3H_3NaO_2$) as polymerizable monomer (Mw $\sim$ 94.04), triethanolamine (TEA) as coinitiator and plasticizer (Mw = 149.19) and sodium salt 5'-riboflavin monophosphate (RF) as sensitizing dye (Mw = 478.33). All compounds were purchased from Merck KGaA (Darmstadt, Germany). The concentration of the compounds in the prepolymer solution has been chosen to obtain thin ($< 200$ $\mu$m) multiplexed holograms with high yields.[15] The prepolymer solution in water was prepared in the laboratory, using a conventional magnetic stirrer, under red light. It was then manually deposited onto leveled glass plates and stored inside an incubator overnight under controlled conditions (60 $\pm$ 5% relative humidity and 20 $\pm$ 1° temperature).

The experimental setup used to record multiplexed HLs was a standard transmission holographic setup[15] in which the interference pattern on the photopolymer was obtained between a collimated and divergent beam, reference and object beam, respectively. The coherent source used was a continuous (CW) diode pumped laser emitting at $\lambda_0 = 473$ nm (Excelsior, Spectra Physics GmbH, Germany) and impinging on the photopolymer with 1.5 mW/cm$^2$ (obtained as the sum of both beams). It was spatially filtered and then split into two secondary beams, the object and reference beams, in a 2:1 ratio. The divergent beam was obtained using a refractive lens (RL) with a dioptric power of 20 D placed at $2f'_{RL}$ distance ($\sim$10 cm) from the photopolymer surface. The object and reference recording angles ($\theta_0$ and $\theta_r$) were measured with respect to the normal of the sample, taking the positive angles clockwise and the negative angles counterclockwise (Figure 1). Both beams were spatially overlapped in the photopolymer layer and the interbeam angle ($\theta = \theta_0 - \theta_r$) was maintained at 14.8° in all recorded holograms, obtaining a low central spatial frequency ($1/\Lambda$) of 545 lines/mm (Equation 1).

$$\Lambda = \frac{\lambda_0}{2\sin\left(\frac{\theta}{2}\right)} \tag{1}$$

The sample was rotated around its vertical axis to record each holographic concentrator composed of seven HLs. Therefore, different object $\theta_0$ and reference angles $\theta_r$ were used in each exposure. The holographic configurations in Figure 1 are characterized by a theoretical $\varphi$, the angle formed between the z-axis (horizontal) and the direction of the propagation vector $\vec{K}$ which is normal to the interferential planes. This parameter is defined by the Equation 2 where the object $\theta'_0$ and the reference angle $\theta'_r$ within the material can be obtained by using the Snell's Law.

$$\varphi = \frac{\theta'_o + \theta'_r}{2} + \frac{\pi}{2} \tag{2}$$

For example, the holographic configuration 1 (C-1) is characterized by the positive object $\theta_0$ and the reference angle $\theta_r$, both clockwise, and its theoretical $\varphi$ will be about 105°; holographic configuration 4 (C-4) corresponds to a symmetrical configuration in which $\theta_0$ and $\theta_r$ are symmetrical with respect to the normal of the plate, in this case $\varphi = 90°$; finally when both recording angle are negative, as configuration (C-7), the slant angle will be inclinated towards the other side, $\varphi = 75°$ (see Figure 1).

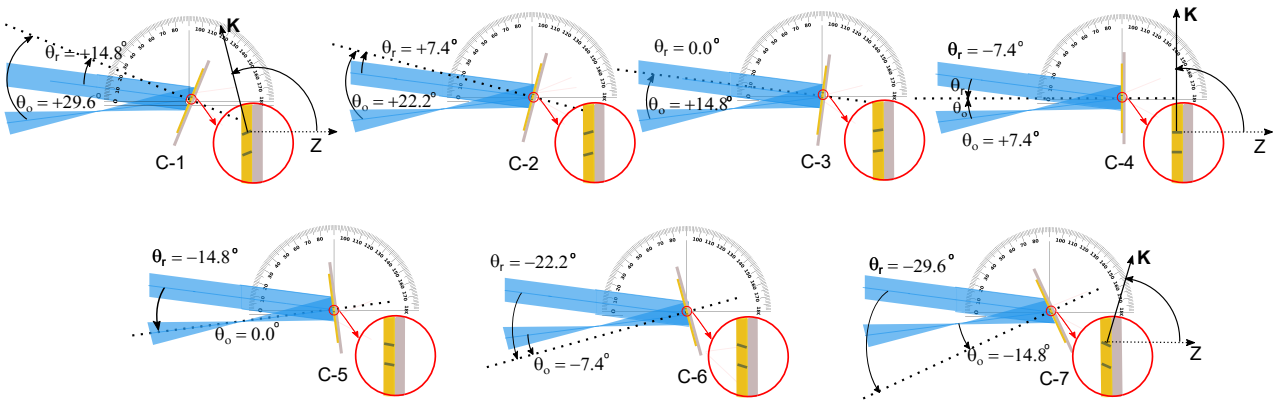


Figure 1. Object and reference angle, $\theta_0$ and $\theta_r$, of the seven overlapping multiplexed holograms. Detail of the inclination of the interferential planes in each configuration (from C-1 to C-7), and detail of theoretical $\varphi$ in C1, C4 and C7.

The four holographic solar concentrators were recorded under safe light conditions (red light). Once the recording process is finished, the remaining dye of the sample is bleached with a white light lamp, a LED lamp (13.5 W, 875 lm at 6500 K, 30° Lexman) placed 37.5 cm from the sample for 5 minutes. Longer photocuring process could provide more transparent concentrators. The physical thickness of the photopolymer layers was measured by using a micrometer screw at the end of the experiments.

## 2.2 Solar characterization setup

Once multiplexed holographic solar concentrators have been stabilized by a photocuring process, they were characterized firstly under red light and secondly under unpolarized broadband source. In both cases it has been used a collimated beam that impinges on the glass substrates (back side of the concentrator) to reconstruct the real image of the HLs with the converging conjugated beam.[15,16] In Figure 2 is represented the sunlight reconstruction of two HLs recorded by using two holographic configurations of Figure 1 a) C-4 and b) C-5. Each configuration is characterized by a different slant, so the more efficient incident angle will be slightly different between them. In Figure 2a the higher diffraction efficiency at 473 nm will be obtained when the sunlight impinge over the sample with $\theta_r = 7.4$ ° with respect to the normal of the plate. While in Figure 2b the higher diffraction efficiency at 473 nm will be obtained when the sunlight impinge over the sample with $\theta_r = 14.8$ ° with respect to the normal of the plate.

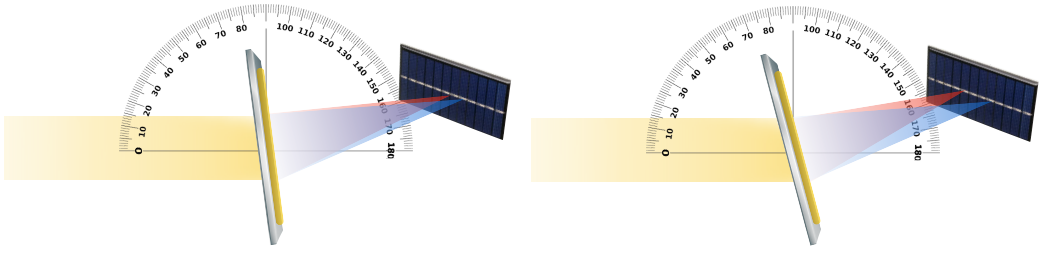

(a) Configuration 4 (C-4). (b) Configuration 5 (C-5).

Figure 2. Bragg incident angle at 473 nm in HL configurations C-4 and C-5. Diffracted angle for blue (473 nm) and red (633 nm) wavelength of the first diffracted order.

To characterize the holographic solar concentrators, two different experiments have been carry out. On the one hand, the diffraction efficiency (Equation 3) has been obtained by measuring the diffracted and transmitted light power at 633 nm.

$$DE = \frac{I_D}{I_D + I_T} \tag{3}$$

On the other hand, the relative value of the short-circuit current under short-circuit conditions ($R = 0\ \Omega$) produced in a PV solar cell (PHIWE 2.5×5 $cm^2$) when illuminated with a broadband collimated light from a solar simulator (model 10500, ABET technologies) has been measured.

## 3. RESULTS

### 3.1 Diffraction efficiency and acceptance angle of multiplexed holographic concentrators

Solar PV concentrator designs, used in solar plants, often require expensive and dynamic solar tracking technologies to concentrate sunlight on solar cells from sunrise to sunset. The most important problem with the use of dynamic solar tracking systems in PV plants is the costly maintenance of mechanical and electronic parts.[17] In addition, the use of huge and extensive solar plants could represent an emerging source of soil consumption, albeit reversible, that impedes the use of soils for agricultural purposes and may affect crucial ecosystem services.[18] Building-Integrated Concentrating Photovoltaic (BICPV) applications installed on home rooftops avoid such problems in the soil ecosystem, but not all rooftops work with standard solar panels. Orientation matters. Versatile HOEs are known to be adaptable to different situations. For example, their spectral selectivity allows them to focus each band frequency at a particular diffracted angle or a particular solar PV cell characterized with a singular bandgap.[19,20] Therefore, versatile multiplexed holographic solar concentrators, which foucs sunlight at different incidence angles are presented in this work as a major challenge in solar energy innovation (Figure 3).

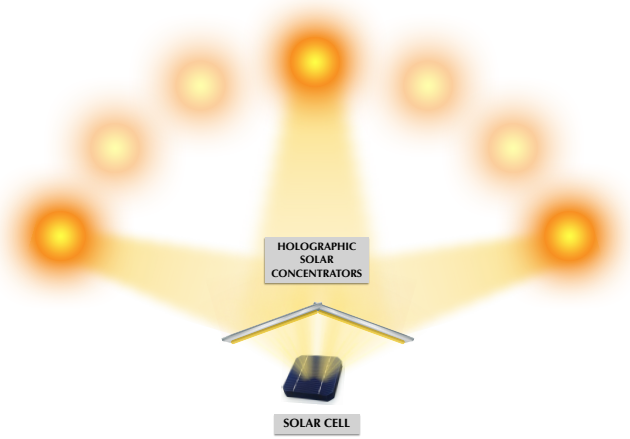


Figure 3. Multiplexed holographic solar concentrator working from sunrise to sunset.

Here we have studied multiplexed HLs with a short focus distance ($f'$), around 5 cm. This focusing distance has been chosen to obtain a high numerical aperture (NA) while maintaining a constant collector area. To obtain a high angular bandwidth with good diffraction efficiency, two strategies can be followed attending to Kogelnik's theory:[21] a) to reduce the film thickness or b) to reduce the spatial frequency. Here we have fabricated HOEs with a center frequency of 545 lines/mm and a film thickness ranging from 134 to 145 $\mu$m. These parameters allow to obtain high efficiency and wide bandwidth in each multiplexed HOE.

As we have shown in Figure 1, the seven multiplexed HLs have been prepared with the same interbeam recording angle, 14.8°. We obtained several holographic configurations by rotating the sample 7.4° and thus modifying the object, the reference angle and the slant in each HL. The multiplexed holographic solar concentrators composed by seven HLs studied in this work are named as HC-m7a, HC-m7b, HC-M7c, HC-m7d, and the particular film thickness of each one after solar characterization are: 134 $\mu$m (HC-m7a), 142 $\mu$m (HC-m7b), 145 $\mu$m (HC-M7c), and 134 $\mu$m (HC-M7d).

The holographic concentrators shown in Figure 4a are denoted HC-m7a and HC-m7b, they have been recorded from configuration 1 (C-1) to configuration 7 (C-7), while the holographic concentrators shown in Figure 4b are denoted HC-m7c and HC-m7d and have been recorded in the opposite direction from C-7 to C-1. In all cases, the exposure is minimal at the beginning and increases in the following recorded HLs. Exposures ranging from 0.8 mJ/cm$^2$ to 142.5 mJ/cm$^2$ have been used to obtain each HL from the four different peristrophic multiplexed holographic concentrators (HC-m7a, HC-m7b, HC-m7c, HC-m7d).

The experimental maximum diffraction efficiency of the four holographic concentrators at 633 nm has been plotted in Figure 4 versus the exposure used in each HL (recorded from C-1 to C-7 or from C-7 to C-1). In all cases we started recording the first HL with a low exposure, 2.3 mJ/cm$^2$ (in the holographic concentrators HC-m7a, HC-m7b), 1.5 mJ/cm$^2$ (HC-m7c), and 0.8 mJ/cm$^2$ (HC-M7d).

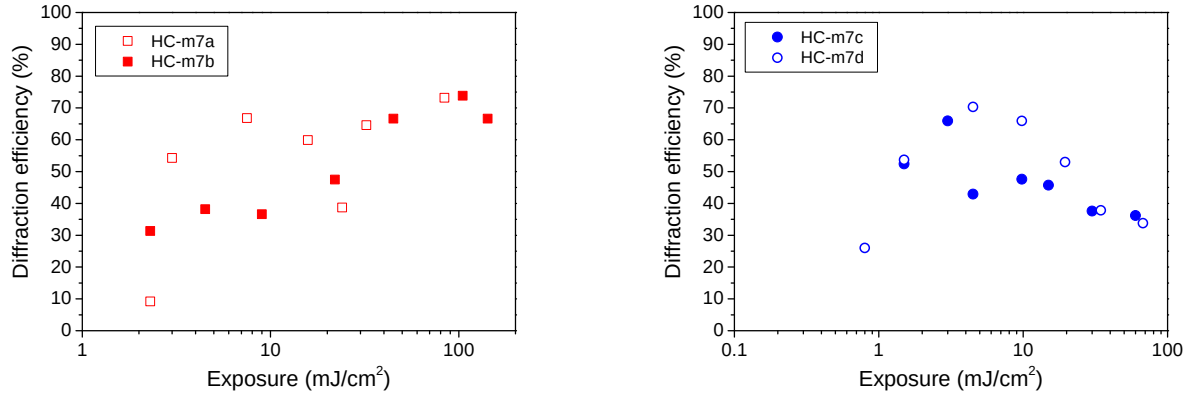


(a) HC-m7 (a, b).

(b) HC-m7 (c, d).

Figure 4. Maximum diffraction efficiency at 633 nm vs exposure at 473 nm of the multiplexed holographic concentrators.

We can observe that the same first exposure in HC-m7a and HC-m7b (Figure 4a) do not produce exactly the same diffraction efficiency value. This could be explained from some inhomogenities in the photopolymer plate that may occur or also by the slightly different thickness between the photopolymer layer of HC-m7a and HC-m7b, which are 134 and 142 $\mu$m, respectively. However, we can observe in both holographic concentrators a quite similar positive trend of diffraction efficiency when the exposure of each hologram is exponentially increased. Finally, a very similar diffraction efficiency values in the last HLs are obtained, around 75%.

In Figure 4b we observe that the maximum diffraction efficiency values increase in the first exposures and then a gradual decrease is observed until very similar diffraction efficiencies are reached between them, around 40%. The variations of maximum diffraction efficiency as a function of the exposure used in each configuration is more significant in the holographic concentrator HC-m7d, while the maximum diffraction efficiency values are most stable in the HC-m7c holographic concentrator. Taking into account the maximum diffraction efficiency values at 633 nm shown in Figure 4, we have decided to analize the relative short-circuit current produced on the solar cell under sunlight with the more efficient holographic solar concentrator (HC-m7b) and the holographic solar concentrator with most stable diffraction efficiency vales (HC-m7c). Both holographic concentrators (HC-m7b and HC-m7c) have a thicker photopolymer layer than HC-m7a and HC-m7d, which are 134 $\mu$m thick after solar characterization.

### 3.2 Sunrise-sunset photovoltaic arrangement

Here we have explored the possibilities offered by holographic technology to achieve customized and breakthrough photovoltaic applications. The relative short-circuit intensity measured with both holographic solar concentrators (HC-m7b and HC-m7c) is plotted in Figure 5 as a function of the angle of incidence of sunlight on the plate. As we can observe, a higher intensity is obtained with HC-m7b in all holographic configurations except to configuration 2 (C-2). The acceptance angle of both holographic concentrators studied are similar, about 130°, although the acceptance angle of HC-m7b is slightly higher than the obtained with HC-m7c.

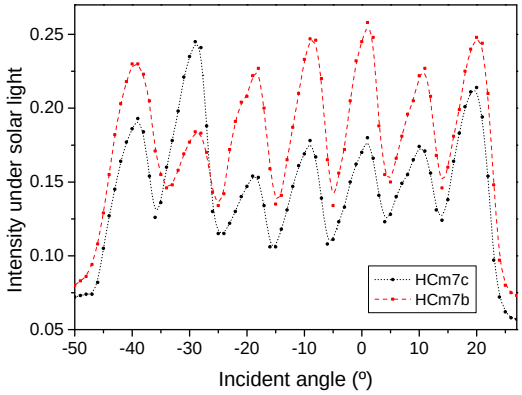


Figure 5. Relative short-circuit intensity measured on the solar cell with HCm7-b and HCm7c under solar light illumination

In any case, the optimal holographic solar concentrator will be chosen according to the particular functionalities required in each system. We can observe that these results open enormous possibilities to produce environmentally friendly holographic solar concentrators, which allow to track sunlight over an acceptance angle of 130° without the need of expensive tracking systems. Moreover, we have verified that the performance of holographic solar concentrators published in (Morales et. al. Opt. Express 30, 25366 (2022) remains almost stable at ambient conditions for more than 15 months. The diffraction efficiency and the relative short-circuit intensity have been maintained, while the acceptance angle has slightly increased (from 120° to 130°), probably explained by the reduction of the film thickness produced by the evaporation of the remaining water inside the photopolymer.

## 4. CONCLUSIONS

In this work, we have explored the possibilities of overcoming the trade-off between good diffraction efficiency at 633 nm and good solar cell performance in two multiplexed holographic solar concentrators focusing sunlight onto it. The peristrophic multiplexed holographic concentrators have been recorded by rotating the sample by half the value of the interbeam recording angle. A larger angular separation will produce smaller minimum short-circuit intensity values, while smaller angular steps between the different holographic configurations will produce a smaller angular acceptance angle. However, the most important challenge of this report is that here we show a versatile method to obtain breakthrough photovoltaic applications. First, we can increase the thickness of the photopolymer to multiplex a larger number of HOEs. Second, we can reduce the spatial frequency of the holograms to increase the bandwidth of each peaks. Third, we have shown how the exposure time selected in each holographic configuration determines the final efficiency in the solar PV cell under sunlight. The presented system allows focusing the sunlight on the photocell with a wide acceptance angle and good efficiency. These results open huge possibilities for producing environmentally fiendly HCs, that follow sun over more than 130° acceptance angle without the need of expensive tracking systems.

## ACKNOWLEDGMENTS

Generalitat Valenciana (CIDEXG/2022/60, IDIFEDER/2021/0.14, PROMETEO/2021/006); Ministerio de Ciencia e Innovación (PID2019-106601RB-I00; PID2021-123124OB-I00); Universidad de Alicante (UAFPU20-23).

## REFERENCES


[1] Arvizu, D., "Development of the sandia 200x experimental silicon module," in [*Seventeenth IEEE Photovoltaic Specialists Conference*], *IEEE Photovoltaic Specialists Conference* **(8)** (1984).

[2] de Jong, T. M., de Boer, D. K. G., and Bastiaansen, C. W. M., "Diffractive flat panel solar concentrators of a novel design," *Optics Express* **24**, 1138–1147 (2016).

[3] Gupta, M., Dubey, A. K., Kuamr, V., and Mehta, D. S., "Indoor daylighting using fresnel lens solar-concentrator-based hybrid cylindrical luminaire for illumination and water heating," *Appl. Opt.* **59**, 5358–5367 (2020).

[4] Kasaeian, A., Tabasi, S., Ghaderian, J., and Yousefi, H., "A review on parabolid trough/fresnel based photovoltaic thermal systems," *Renewable and Sustainable Energy Reviews* **91**, 193–204 (2018).

[5] Kumar, V., Shrivastava, R. L., and Untawale, S. P., "Fresnel lens: A promising alternative of reflectors in concentrated," *Renewable and Sustainable Energy Reviews* **44**, 376–390 (2015).

[6] Vorndran, S. H., Chrysler, B., Wheelwright, B., Angel, R., Holman, Z., and Kostuk, R., "Off-axis holographic lens spectrum-splitting photovoltaic system for direct and diffuse solar energy conversion," *Applied Optics* **55**, 7522–7529 (2016).

[7] Russo, J. M., Castillo, J. E., Aspnes, E., Kostuk, R. K., and Rosengerg, G., "Daily and seasonal performance of angularly dependent fixed mount dual aperture holographic planar concentrator photovoltaic modules," *SPIE* **7769**, 1–9 (2010).

[8] Bañares-Palacios, P., Álvarez Álvarez, S., Marín-Sáez, S., Collados, J., and Chemisana, M. V., "Broadband behaviour of transmission volume holographic optical elements for solar concentration," *Opt. Express* **23**, A671 (2015).

[9] Navarro-Fuster, V., Ortuño, M., Fernández, R., Gallego, S., Márquez, A., Beléndez, A., and Pascual, I., "Peristrophic multiplexed holograms recorded in a low toxicity photopolymer," *Opt. Mater. Express* **7**, 133–147 (2017).

[10] Fernández, R., Bleda, S., Gallego, S., Neipp, C., and A. Márquez, Y. Tomita, I. P. A. B., "Holographic waveguides in photopolymers," *Optics Express* **27**, 827–840 (2019).

[11] Lee, J. H., Wu, Y., Piao, M., and Kim, N., "Holographic solar energy concentrator using angular multiplexed and iterative recording method," *IEEE Photonics J.* **8**, 1–11 (2016).

[12] Akbari, H., Naydenova, I., Ahmed, H., McCormack, S., and Martin, S., "Development and testing of low spatial frequency holographic concentrator elements for collection of solar energy," *Sol. Energy* , 103–109 (2017).

[13] Kao, H., Ma, J., Wang, C., Wu, T., and Su, P., "Crosstalk-reduced double-layer half-divided volume holographic concentrator for solar energy concentration," *Sensors* **20**, 6903 (2020).

[14] Wang, C., Ma, J., Kao, H., Wu, T., and Su, P., "Wide-band high concentration-ratio volume-holographic grating for solar concentration," *Sensors* **20**, C1 (2020).

[15] Morales-Vidal, M., Lloret, T., Ramírez, M. G., Beléndez, A., and Pascual, I., "Green and wide acceptance angle solar concentrators," *Optics Express* **30**, 25366–25378 (2022).

[16] Lloret, T., Navarro-Fuster, V., Ortuño, M. G., Neipp, C., Beléndez, A., and Pascual, I., "Holographic lenses in an environment-friendly photopolymer," *Polymers* **10**, 302 (2018).

[17] Wiesenfarth, M., Anton, I., and Bett, A. W., "Challenges in the design of concentrator photovoltaic (cpv) modules to achieve highest efficiencies," *Applied Physics Reviews* , 041601 (2018).

[18] Moscatelli, M. C., Marabottini, R., Massaccesi, L., and Marinari, S., "Soil properties changes after seven years of ground mounted photovoltaic panels in central italy coastal area," *Geoderma Regional* **33**, e00500 (2022).

[19] Darbe, S., Escarra, M. D., Warmann, E. C., and Atwater, H. A., "Simulation and partial prototyping of an eight-junction holographic spectrum-splitting photovoltaic module," *Energy Science Engineering* **7**, 2572–2584 (2019).

[20] Khan, A. A. and Yadav, H. L., "Dichromated gelatin, an efficient material for the fabrication of wavelength selective holographic solar concentrators for high-efficiency operation," *Material Today: Proceedings* **56**, 94–99 (2022).

[21] Kogelnik, H. and Shank, C. V., "Coupled-wave theory of distributed feedback lasers," *J. Appl. Phys.* **43**, 2327–2335 (1972).